Spectroscopy of optical counterparts of ultraluminous X-ray sources

Abolmasov P., Fabrika S., Sholukhova O., Afanasiev V.

Special Astrophysical Observatory of the Russian AS, Nizhnij Arkhyz 369167, Russia

Abstract. Here we present the results of panoramic and long-slit observations of eight ULX nebular counterparts held with the 6m SAO telescope. In two ULXNe we detected for the first time signatures of high excitation ([O III]λ5007 / H$\beta > 5$). Two of the ULXs were identified with young ($T \sim 5 - 10\ Myr$) massive star clusters. Four of the eight ULX Nebulae (ULXNe) show bright high-excitation lines. This requires existence of luminous ($\sim 10^{38} \div 10^{40}$ergs s^{-1}) UV/EUV sources coinciding with the X-ray sources. Other 4 ULXNe require shock excitation of the gas with shock velocities of 20-100$km\,s^{-1}$. However, all the studied ULXN spectra show signatures of shock excitation, but even those ULXNe where the shocks are prevailing show presence of a hard ionizing source with the luminosity at least $\sim 10^{38}$ergs s^{-1}. Most likely shock waves, X-ray and EUV ionization act simultaneously in all the ULXNe, but they may be roughly separated in two groups, shock-dominated and photoionization-dominated ULXNe. The ULXs have to produce strong winds and/or jets powering their nebulae with $\sim 10^{39}$ergs s^{-1}. Both the wind/jet activity and the EUV source needed are consistent with the suggestion that ULXs are high-mass X-ray binaries with the supercritical accretion disks of the SS433 type.

Key words: Ultraluminous X-ray sources – optical spectroscopy – nebulae

1. Introduction

1.1. Ultraluminous X-ray Sources

A point-like X-ray source is considered an Ultraluminous X-ray Source (ULX) if its luminosity exceeds $10^{39} erg\,s^{-1}$ and it does not coincide with the galactic nucleus (to exclude active galactic nuclei). There are more than 150 ULXs known at the present time (Swartz, 2004) but very little is clear yet about the physical nature of these objects.

Luminosity of an accreting source is limited by the Eddington value, that for a stellar mass ($\sim 10 M_\odot$) black hole is about 10^{39}ergs s^{-1}. The limit, however, can be violated by a logarythmic factor if accretion is supercritical (Shakura & Sunyaev, 1973; Abramowicz et al., 1980). ULXs most likely are accreting black holes (their compactness follows from relatively fast variability of some of them (Krauss et al., 2005; Soria et al., 2006)), and their apparent luminosities are well above the Eddington limit for a stellar mass ($\sim 10 M_\odot$) black hole. Different models were proposed to explain the ULX phenomenon, basing on three main ideas:

- the black hole mass may be larger, $\sim 100 - 10000$ solar masses, – Intermediate Mass Black Holes, IMBHs (Madau & Rees, 2001; Colbert & Miller, 2005)

- accretion may be supercritical but still radiatively efficient (Begelman, 2002)

- observed source may be intrinsically anisotropic (Fabrika & Mescheryakov, 2001; King et al., 2001)

IMBHs are supposed to accrete matter from massive donor stars, accretion from interstellar medium is unlikely to provide enough material. Possible observational appearences of IMBH+donor close binaries were considered by Hopman et al. (2004) and Copperwheat et al. (2005). IMBHs are considered either compact remnants of Population III stars (Madau & Rees, 2001) or products of stellar collisions in stellar cluster or protocluster cores (Soria, 2006).

Supercritical accretion disks (SCADs) are the most appreciated alternative to the scenarios involving IMBHs. The best candidates are massive black-hole binaries like SS433, the only example of a supercritical accretor in the Galaxy (Fabrika, 2004).

1.2. Optical Counterparts

For most of the well-studied ULXs optical counterparts were found. In some cases optical observations reveal stellar counterparts – usually OB supergiants (Liu et al., 2001; Terashima et al., 2006). Many of ULXs are situated inside star-forming regions and therefore they are heavily absorbed (Terashima et al.,

2006).

Large number of ULXs are located inside nebulae (ULX nebulae, ULXNe), sometimes superbubbles more than hundred parsecs in size (Pakull & Mirioni, 2003; Pakull et al., 2006), usually having spectra typical for shock-powered nebulae (bright [S II]λ6717,6731, [N II]λ6748,6583, [O I]λ6300,6364 and [N I]λ5200 lines). In some cases the appearence of a ULXN may be quite different, like the high-excitation photoionized H II region of HoII X-1 (Lehmann et al., 2005) or a compact very bright shell-like nebula with anomalous excitation conditions (the nebula MF16, (Abolmasov et al.2006; Abolmasov et al.2007a)).

One of the interesting properties of some ULXNe is He IIλ4686 emission line. Due to this reason, ULXNe were considered X-ray Ionized Nebulae (XINe, Pakull & Mirioni, 2003). This is often considered an argument for truely large X-ray luminosities of ULXs (Kaaret et al., 2004). However, extreme ultraviolet radiation in the wavelength range $\lambda \sim 100 - 200\mathring{A}$ has larger ability for producing He IIλ4686 recombination emission line than X-rays. Therefore nebulae like MF16 and that around HoII X-1 may be not X-ray Ionized Nebulae. For more details see discussion in Abolmasov et al. (2007a). In some cases like HoIX X-1 and NGC1313 X-1 (Grisé et al., 2006; Pakull et al., 2006) the HeII emission is broadened by $\sim 1000 km\, s^{-1}$ and can be produced either in the accretion disk or in a Wolf-Rayet donor atmosphere.

Many of ULXs are located close to young stellar clusters, often at tens to hundreds parsecs from the clusters or groups of massive stars (Zezas et al., 2002). There are numerous indications for the ULXs are related to young (5-10 Myr) stellar population (Soria et al., 2005; Zezas et al., 2002; Abolmasov et al., 2007b). For distant ULXs ($D \gtrsim 15$ Mpc) bright star clusters with surrounding nebulae become the only association available for optical studies.

In the following section 2 we describe our observations of ULX counterparts with the 6m BTA telescope. In section 3 results of the spectral analysis and modelling of the optical counterparts are presented. In section 4 we discuss the inference on the nature of ULXs which may follow from the observations of the ULXNe.

2. Observations and Data Reduction

We have focused on targets with known optical counterparts, situated in nearby galaxies ($D \lesssim 10 Mpc$). The only exception is NGC7331 X-1, but in that case a bright host cluster of $V \sim 20^{\rm m}$ is present. All the host galaxies are of late Hubble types. In table 2 we list the ULX counterparts observed. We used accurate Chandra X-ray coordinates ($\pm 0.3''$) according to Swartz et al.(2004), Roberts et al.(2003) in the case of IC342 X-1, Terashima & Wilson (2004) in the case of M51 X-7 and Mescheryakov (2004) for HoIX X-1.

All the data were obtained with two spectrographs: Multi-Pupil Fiber Spectrograph MPFS (Afanasiev et al., 2001) and SCORPIO (Afanasiev & Moiseev, 2005) focal reducer in long-slit mode. 3D data have the advantage of providing unbiased flux calibrations. However, SCORPIO has higher quantum efficiency by a factor of up to ~ 6.

MPFS was used with the grating # 4 (600 lines/mm), SCORPIO was used with grisms VPHG550G and VPHG1200G. Spectral ranges and spectral resolutions are listed in table 2. Seeing conditions during observations were from 1 to $2''$. For the long-slit observations we estimate the light losses on the slit, consistent with the actual seeing value. For the sources listed in table 2 we have obtained either long-slit or panoramic spectra appropriate for analysis.

Data reduction system was written in IDL6.0 environment, using procedures written by V. Afanasiev, A. Moiseev and P. Abolmasov. For long-slit observations the reduction system contains all the standard procedures. For 3D data the standard procedures for panoramic data reduction were used (i. e. those standard for long-slit data plus extraction of fiber spectra and fiber sensitivity calibration). For MPFS data atmospheric dispersion correction was made with accuracy $\sim 0''.1$.

In all the targets emission lines from the surrounding nebulae were detected. Contribution from the stellar continua (host cluster or association) has also been detected in some cases. Emission line parameters were calculated using gauss analysis. Fitting by two gaussians was used for [SII]$\lambda\lambda$6717,6731 doublet, Hγ+[OIII]λ4363, HeII λ4686+FeIIIλ4658 and FeII+FeIII λ5262,5270 blends, triple gaussian was used to deblend Hα with [NII]λ6548,6583 doublet (for the components of the latter both fixed wavelength difference and flux ratio $F(\lambda 6583/\lambda 6548) = 3$ were adopted). Exact wavelength values with an accuracy of $\sim 0.1\mathring{A}$ were taken from Coluzzi (1996).

Among our targets there are two large-scale bubble nebulae (HoIX X-1 and IC342 X-1) and four high-excitation nebulae (HoII X-1, NGC6946 ULX-1, M101 P098 and NGC5204 X-1) In two cases (M51 X-7 and NGC7331 X-1) comparatively high S/N cluster spectra with nebular contribution where obtained.

3. Results and Interpretation

Emission line integral fluxes and luminosities are given in table 2. In the last row we estimate the total power of the nebula suggesting it either a shock-powered (see section 3.1) or photoionized HII region (see section 3.2).

Table 1: *Observed ULXs. The columns present the target IDs, ULX X-ray coordinates (JD 2000), distances D to the host galaxies in Mpc, Galactic absorption A_V in the source direction according to Schlegel (1998), angular distances R of targets towards the center of their galaxies in arcminutes, oxygen abundances according to Pilyugin et al. (2003) (the central abundance, but interpolated abundances to the target angular distance from the center are given in brackets), comments on the optical counterparts, exposure time in seconds, spectral range in Å, spectral resolution in Å, in the MPFS oservations and the same parameters in the SCORPIO observations.*

object ID	RA, h,m,s	Dec, ° ′ ″	D	A_V	$R,'$	$12+\lg(O/H)$	optical counterpart	MPFS observations			SCORPIO observations		
								t_{exp}	sp. range	res.	t_{exp}	sp. range	res.
IC342 X-1	03 45 55.68	+68 04 54.9	3.28[a]	1.51	14.86	8.85 (8.25)	shock-powered nebula (Roberts et al., 2003), $\sim 100pc$	6900	4000-6900	5	7200	3900-5700	5
HoII X-1	08 19 28.99	+70 42 19.4	3.39[b]	0.105	13.74	7.92	HII region with strong HeIIλ4686 emission (Lehmann et al., 2005)	1800	4000-6900	5		—	
HoIX X-1	09 57 53.28	+69 03 48.4	3.7[b]	0.261	16.06	[Fe/H]=-0.4÷-0.7[c]	bubble nebula MH9/10, 200×400 pc (Miller, 1995)	4500	4000-6900	5	1200	3460-7460	10
NGC5204 X-1	13 29 38.62	+58 25 05.6	4.5[d]	0.04	1.96	—	several blue stars and nebular emission (Liu et al., 2004)	8400	4000-6900	5	2700	3900-5700	5
M51 X-7	13 30 00.99	+47 13 43.9	8.4[e]	0.117	30.85	8.92 (6.72)	cluster with offset nebular emission	3600	4000-6900	5		—	
M101 P098	14 03 32.40	+54 21 03.1	7.2[f]	0.029	2.54	8.8 (8.64)	high-excitation nebula	4500	4000-6900	5		—	
NGC6946 X-1	20 35 00.75	+60 11 30.9	5.5[g]	1.141	33.31	8.7 (7.09)	peculiar nebula MF16 (Blair et al., 2001)	5830	4000-6900	5	5400	3900-5700	5
NGC7331 X-1	22 37 06.75	+34 26 17.6	15.1[h]	0.301	19.79	8.68 (7.02)	young star cluster + HII region P98 (Petit, 1998)		—		2700	3460-7460	10

[a] Saha et al.(2002)
[b] Karachentsev et al.(2002)
[c] Tully (1988)
[d] Tully et al.(1992)
[e] Feldmeier et al.(1997)
[f] Stetson et al.(1998)
[g] Hughes et al.(1998)
[h] Makarova et al.(2002)

Table 2: *Observed Hβ fluxes, emission-line fluxes in Hβ units and unreddened luminosities of the ULXNe. For NGC6946 X-1, HoII X-1, M101 P098 and NGC5204 X-1 the luminosities were unreddened using Hα/Hβ criterion and Cardelli et al.(1998) reddening curves. For NGC7331 X-1 the best-fit interstellar absorption ($A_V = 1^{\rm m}.4$) was derived from the stellar population spectrum fit. In other ULXNe the galactic A_V was used (compare with table 2. In NGC7331 X-1 the luminosities in residual emissions are given in brackets (see text for details). The total power estimates for HoII X-1, NGC6946 X-1, M101 P098 and NGC5204 X-1 are hydrogen-ionizing luminosities derived in assumption that Hβ is a recombination line (see section 3.2). Remaining nebulae are treated as shock-powered, their total powers were estimated using equation (3).*

	HoII X-1	NGC6946 X-1	HoIX X-1	IC342 X-1	NGC7331 X-1	M101 P098	NGC5204 X-1	M51 X-7
F(Hβ), 10^{-15}ergs cm^{-2} s^{-1}	11	4.66±0.13	12.6±0.6	4.3±0.08	1.52±0.07	0.5±0.2	1.0±0.3	0.67±0.13
A_V	0.19	1.34	0.26	1.51	1.40	0.41	1.22	0.12
Hδ	–	0.16±0.13	0.40±0.15	–	0.05±0.07	—	—	—
Hγ	0.45	0.381±0.015	0.31±0.10	0.28±0.02	0.34±0.02	—	—	—
[O III]λ4363	0.08	0.174±0.019	0.133±0.15	—	0.03±0.01	—	—	—
He Iλ4471	0.08	0.06±0.06	–	0.051±0.015	—	3±1	—	0.6±0.5
He IIλ4686	0.14	0.170±0.015	0.06±0.02	0.036±0.015	—	—	—	—
He Iλ4713	0.01	—	–	–	—	—	—	—
He Iλ4922	0.01	—	–	–	—	—	—	—
[O III]λ4959	1.00	2.25±0.05	0.537±0.06	0.219±0.015	0.35±0.04	1.7±0.3	2.0±0.2	0.47±0.14
[O III]λ5007	3.00	7.06±0.06	1.47±0.04	0.837±0.016	1.15±0.05	5.6±0.3	5.8±0.3	0.92±0.16
[N I]λ5200	—	0.15±0.05	0.07±0.03	0.302±0.014	0.08±0.04	0.3±0.1	—	—
He IIλ5412	0.02	0.14±0.05	—	—	—	—	—	—
[N II]λ5755	—	0.118±0.15	0.04±0.02	–	0.02±0.03	—	—	—
He Iλ5876	0.07	0.11±0.02	0.17±0.04	2.6±0.4	0.13±0.04	—	—	—
([O I]λ6300+ [S III]λ6310)	0.11	1.42±0.08	0.92±0.14	2.3±0.4	0.15±0.04	—	—	—
[O I]λ6364	0.03	0.48±0.03	0.34±0.06	0.50±0.15	0.02±0.02	—	—	—
Hα	3.20	4.728±0.087	3.79±0.10	5.8±0.1	6.375±0.009	3.45±0.10	4.5±0.5	5.18±0.10
[N II]λ6583	0.08	4.16±0.08	1.18±0.08	4.5±0.1	2.00±0.01	1.24±0.10	0.6±0.1	2.9±0.2
He Iλ6678	0.03	0.06±0.03	∼1?	0.2±0.1	0.04±0.03	—	—	—
[S II]λ6717	0.32	2.46±0.02	1.73±0.04	3.6±0.2	0.97±0.02	0.6±0.2	1.6±0.3	1.29±0.15
[S II]λ6731	0.29	2.35±0.02	1.2±0.04	2.6±0.2	0.71±0.02	0.6±0.3	1.1±0.3	0.97±0.18
Luminosities, 10^{37}ergs s^{-1}:								
HeIIλ4686	0.22	1.31±0.10	0.07±0.02	0.1±0.02	$\lesssim 1$	$\lesssim 0.2$	$\lesssim 0.1$	
Hβ	1.67	7.2±0.3	2.73±0.13	3.3±0.6	21.45±0.19 (6.9)	0.3±0.1	0.9±0.1	0.6±0.1
[O III]λ5007	5.01	48±3	3.97±0.12±	1.4±0.3	19.72±0.19 (12.7)	1.7±0.5	5±1	0.6±0.1
[S II]λ6717,6731	1.02	35±1	7.3±0.4	10.5±0.5	18.2±0.5 (17.2)	0.4±0.2	1.6±0.5	1.4±0.2
Total power	70	500	300	300	(700)	12	60	70

3.1. Bubble nebulae

We classify HoIX X-1 MH9/10 nebula and IC342 X-1 nebula as purely shock-powered nebulae, with the shock velocities in the range $20-100 km\,s^{-1}$. Both estimates follow from the kinematical data, however, in this paper we concentrate on emission line intensities and diagnostics, leaving kinematical studies to further papers. If one suggests photoionisation for these two ULXNe, a source with $L \gtrsim 10^{42}$ ergs s^{-1} is required. Their positions on ionization diagrams (see Fig. 4) are consistent with shocks of moderate power ($V_S \sim 100 km\,s^{-1}$). The total power of a nebula and the mean shock velocity (in the case when the physical size is known) can be estimated using its total Hβ luminosity. According to Dopita & Sutherland (1996), total energy flux in a shock wave:

$$F_{tot} = 2.28 \times 10^{-3} V_2^3 n_0\, erg\, cm^{-2} s^{-1} \quad (1)$$

where V_2 is the shock velocity in 100 $km\,s^{-1}$ units, n_0 is the pre-shock hydrogen density in cm^{-3}. For the energy flux in Hβ:

$$F_{H\beta} = F_{H\beta,shock} + F_{H\beta,precursor} = \left(7.44 \times 10^{-6} V_2^{2.41} + +9.86 \times 10^{-6}\, V_2^{2.28}\right)\, n_0\, erg\, cm^{-2} s^{-1}, \quad (2)$$

$F_{H\beta,shock}$ represents the emission of the cooling material behind the shock, $F_{H\beta,precursor}$ is the contribution of the precursor. The $F_{H\beta,shock}$ term is appropriate for any steady one-dimensional shock but the precursor term goes to zero at $V_S \lesssim 150 km\,s^{-1}$. Combining (1) and (2) one expresses the Hβ luminosity as a function of the total shock power and shock velocity:

$$L_{H\beta} = \left(3.26 \times 10^{-3}\, V_2^{-0.59} + +4.32 \times 10^{-3}\, V_2^{-0.72} \Theta(V_2 - 1.5)\right) L_{tot} \quad (3)$$

where $\Theta(x) = 1$ if $x \geq 0$ and $\Theta(x) = 0$ otherwise. From this equation the total power can be roughly estimated as $L_{tot} \sim (100 \div 300) L_{H\beta}$.

In SCORPIO spectra of MH9/10 we detect roughly a point-like He IIλ4686 emission (figure 1) close to the blue knot (central star cluster of the bubble) and the X-ray source (Grisé et al., 2006). In figure 2 we present 1D maps of the X-ray source vicinity demonstrating that the He II line is emitted at the edge of the central cluster. We estimate the luminosity of the He IIλ4686 source as $\sim (2 \div 4) 10^{36}$ergs s^{-1}(the obtained value was multiplied by a factor $2-4$ estimating the losses of the slit). This is consistent with the results obtained by Grisé et al. (2006), who also detect the He II emission.

In HoIX X-1 nebula this line may have stellar origin. Possible sources of bright He IIλ4686 lines are Wolf-Rayet stars (Conti et al., 1983) and accretion disks. For WN stars the equivalent width can reach 400Å. V-band luminosity is about $10^{37} \div 10^{38}$ergs s^{-1}for bright WN stars, so one WN star can be enough to explain the He IIλ4686emission.

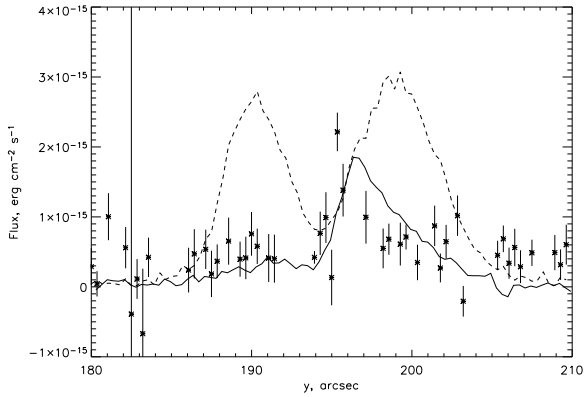

Figure 2: *1D maps for MH9/10 nebula (HoIX X-1) derived along the slit in continuum (solid line; integrated over the wavelength range* $4000-7000Å$*, emission lines excluded by median smoothing), Hα (dashed line) and He* II*λ4686 (asterisks with error bars).*

Bright emission lines in the IC342 X-1 nebula spectrum argue for shock excitation. However, its integral spectrum (figure 3) containes relatively faint high-excitation lines like He II and [Fe III] emitted in the inner parts of the nebula. High-excitation spectrum resembles that of MF16 (see next section).

3.2. NGC6946 X-1

NGC6946 X-1 is known to coincide with a peculiar nebula MF16, for a long time considered a luminous Supernova Remnant (SNR). It is the most compact (20pc×34pc) and one of the brightest among the ULXNe. Its integral spectrum is characterised by the highest [O III]λ5007/Hβ and [N II]λ6583/Hα ratios.

The velocity gradients and non-gaussian structure of the emission lines in our spectra suggest expansion velocity not greater than $200 km\,s^{-1}$. Dunne et al.(2000) have resolved Hα, [N II] and [O III] lines in a narrow (FWHM∼20-40$km\,s^{-1}$) component from unshocked material and a broad (FWHM∼250$km\,s^{-1}$) from shocked material. Basing on the MPFS and SCORPIO spectra we performed a thoroughful analysis of the ionization and excitation sources of the nebula (Abolmasov et al., 2006; Abolmasov et al., 2007a), leading to a conclusion that most of the power of the nebula comes not from shock waves but from photoionizing ultraviolet source even more luminous than the central X-ray source. CLOUDY modelling gives the parameters of the central source in the suggestion that the ionizing continuum in the EUV/UV is a black body: $T = 10^{5.15 \pm 0.15} K$, $L_{BB} = (7.5 \pm 0.5) \times 10^{39}$ergs s^{-1}. For the EUV luminosity one can make rough, but universal estimates (the

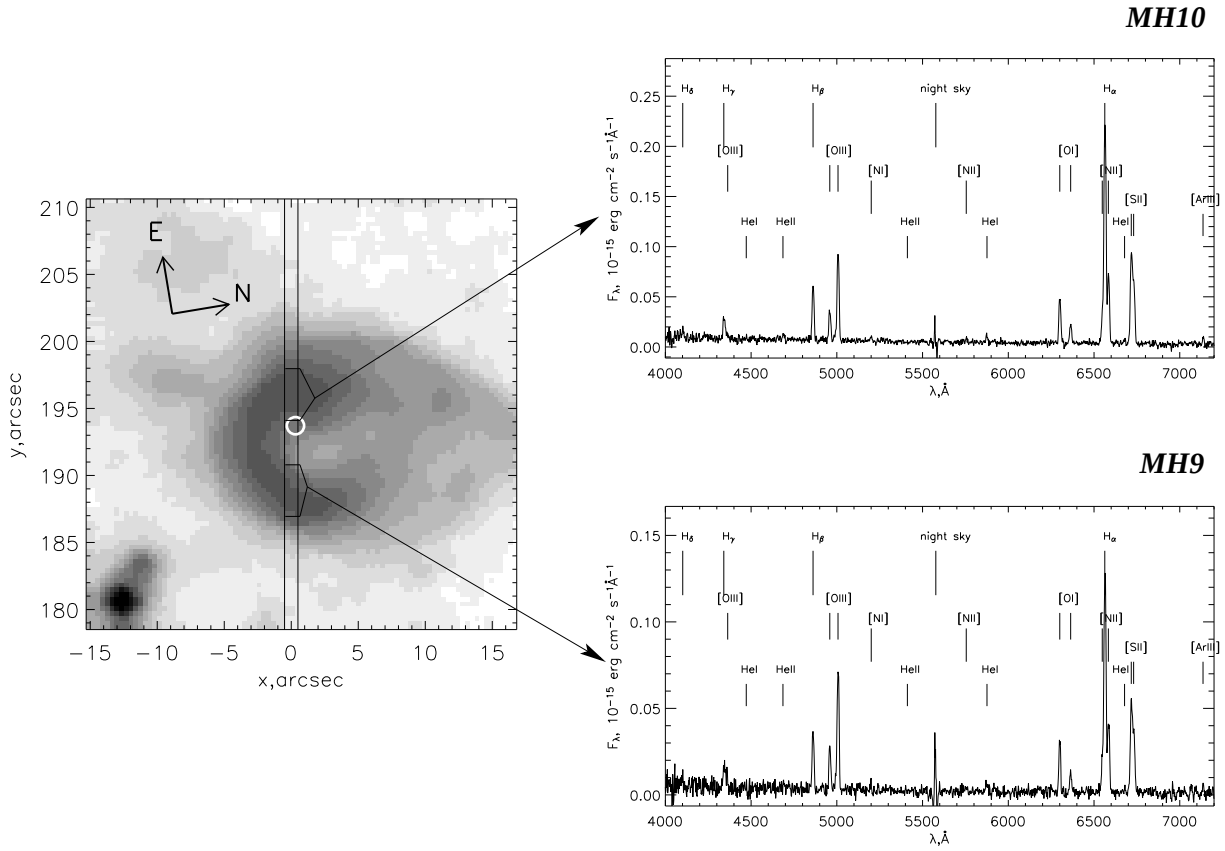

Figure 1: *MH9/10 (the nebula associated with HoIX X-1) Hα image (taken with SCORPIO) with the 1″ slit. The X-ray source coordinates are marked by a white circle. To the right the spectra of the two parts of the nebula known as MH9 (bottom-right panel) and MH10 (top-right panel). In the upper spectrum He* II *λ4686 emission was detected.*

lower limits), based on the ionizing quanta numbers. If He IIλ4686 and Hβ are purely recombination lines one can apply the relations by Osterbrock (1974):

$$L(\lambda < 228\mathring{A}) \geq \frac{4\mathrm{Ry}}{E(\lambda\,4686)} \frac{\alpha_B(He^{++})}{\alpha^{eff}_{HeII\;\lambda 4686}} \times L_{HeII\lambda\,4686} \simeq \simeq 100\, L_{HeII\lambda\,4686} \quad (4)$$

$$L(\lambda < 912\mathring{A}) \geq \frac{1\mathrm{Ry}}{E(H\beta)} \frac{\alpha_B(H^+)}{\alpha^{eff}_{H\beta}} \times L_{H\beta} \simeq 65\, L_{H\beta}, \quad (5)$$

Here α_B values are total recombination rates for the Case B (optically thick to ionizing quanta) for hydrogen and ionized helium, correspondingly. $\alpha^{eff}(line)$ is the effective recombination rate with the particluar emission line quanta production. $\alpha_B(He^{++})/\alpha^{eff}_{HeII\;\lambda 4686}$ and $\alpha_B(H^+)/\alpha^{eff}_{H\beta}$ ratios depend weakly on the plasma parameters. The former changes by about factor of two in the temperature range $(0.3 \div 10) \times 10^4 K$, the latter by about 20%.

In table 2 we give the hydrogen-ionizing luminosities defined this way as estimates for the power of photoionized nebulae. Hβ line can overestimate the photoionizing flux because contribution from shocks may be significant. Discussion about the nature of the EUV photoionizing source follows in section 4.2.

High signal-to-noise spectrum of MF16 obtained with SCORPIO shows numerous high-excitation lines like [Fe III] and Ar IV. Integral spectrum is shown in figure 5.

3.3. High-Excitation ULXNe

In the vicinity of two of the observed sources (M101 P098 and NGC5204 X-1) we detect regions with high [O III]λ5007/Hβ ratio (> 5). They can be seen as bright spots on the [O III]λ5007 flux maps shown in figure 6. The [O III]λ5007/Hβ ratios are similar to that of MF16, but the integral luminosities are much less – an order of magnitude less for NGC5204 X-1 and even more for M101 P098.

M101 P098 nebula is well resolved as an elongated region $1'' \times 4''$, bright in [O III]λ5007,4959 lines (see figure 6a). For the distance 7.2 Mpc this corresponds to the physical size about $35pc \times 140pc$.

Bright [O III]emission lines argue for either a photoionizing source capable to provide ionization pa-

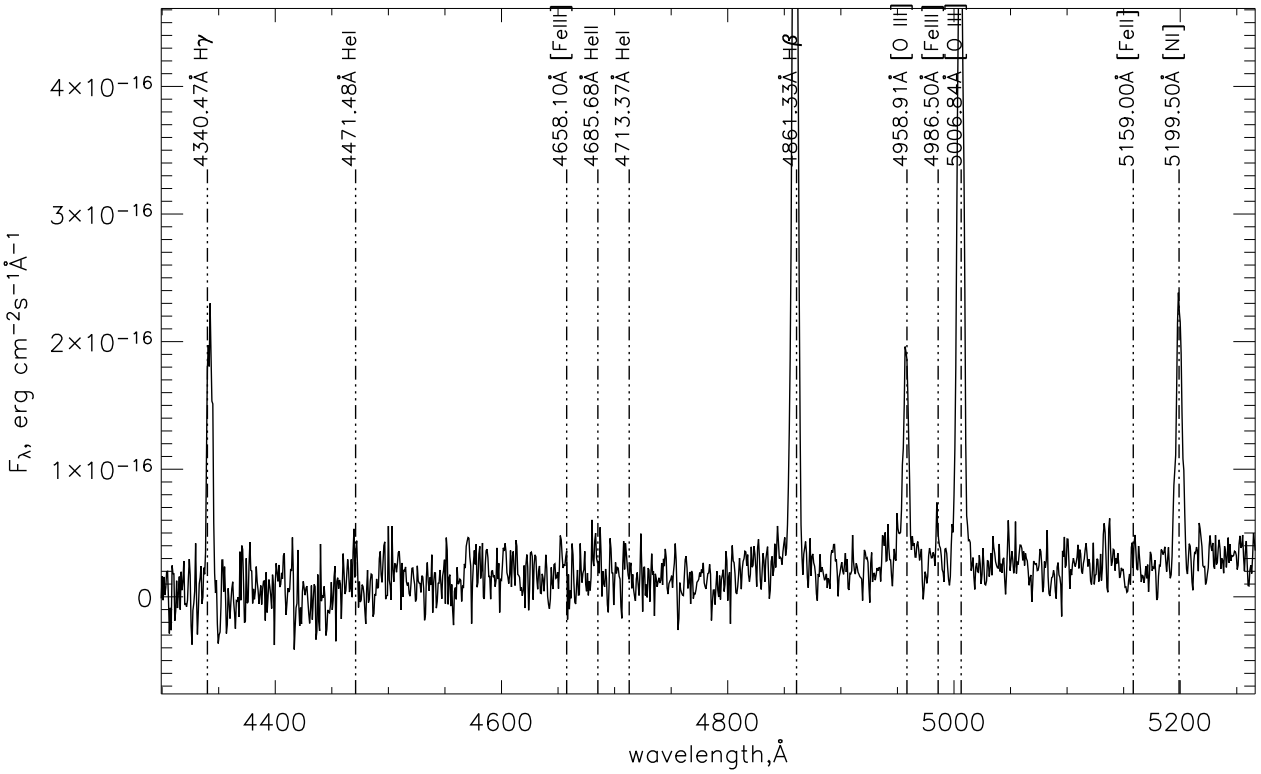

Figure 3: *Spectrum of the IC342 X-1 nebula (SCORPIO). The He* II *λ4686 emission originates roughly in the center of the ULXN.*

rameter[1] $\gtrsim 10^{-3}$ at about 50 pc or shock waves with $V_S \gtrsim 300 km\,s^{-1}$ propagating at similar spatial scales (Evans, 1999; Dopita & Sutherland, 1996). Photoionizing source must have the hydrogen-ionizing luminosity $\gtrsim 2 \times 10^{38}$ergs s^{-1}, so M101 P098 can be considered an analogue of MF16 in a more rarefied ISM. From the other hand, fast shocks with $V_S \sim 300 - 500 km\,s^{-1}$ require practically identical power $(1.5 - 2) \times 10^{38}$ergs s^{-1} to provide the observed Hβ luminosity. The example of MF16 suggests that these high-excitation nebulae are more likely to be photoionized HII regions. However, both photoionization and shock excitation can act in powering these nebulae.

HoII X-1 is another example of a high-excitation ULX nebula. [O III]λ5007/H$\beta \sim 3$ is low if compared with the M101 P098 and NGC5204 X-1 spectra, but HoII has lower oxygen abundance, so the physical conditions may be quite similar. He IIλ4686 emission line is very bright relative to Hβ ($F(HeII\lambda4686)/F(H\beta) \sim 0.2$), but the total luminosity in this line is an order of magnitude lower than that in MF16. Our results on this object were published in Lehmann et al.(2005). Long-slit spectrum (obtained with UAGS spectrograph) of the nebula is shown in figure 7.

3.4. Star Clusters

Among the observed ULXs two objects coincide with isolated bright star clusters: NGC7331 X-1 and M51 X-7. Among the other ULXs whose X-ray boxes contain stellar clusters, there are HoIX X-1 (the cluster is very faint, $V \sim 20^{\rm m}.5$ and not massive) and NGC5204 X-1 (the cluster is a part of a more complex star-forming region).

A nearly point-like continual source is seen in ground-based images of the NGC7331 X-1 region. At the distance of 15 Mpc its size is $\sim$ 50 pc. In the HST images the source consists of young cluster and some fainter sources around (Abolmasov et al., 2007b). The cluster coincides with the HII region P98 (Petit, 1998). Our study of the source environment based on *HST* and SCORPIO observations is published in a separate paper (Abolmasov et al., 2007b). We fitted the integral spectrum of the stel-

[1] We define ionization parameter as (for example, in Evans et al.(1999)):

$$U = \frac{1}{cn}\int_{13.6eV}^{+\infty} \frac{F_E}{E} dE,$$

where n is the gas number density.

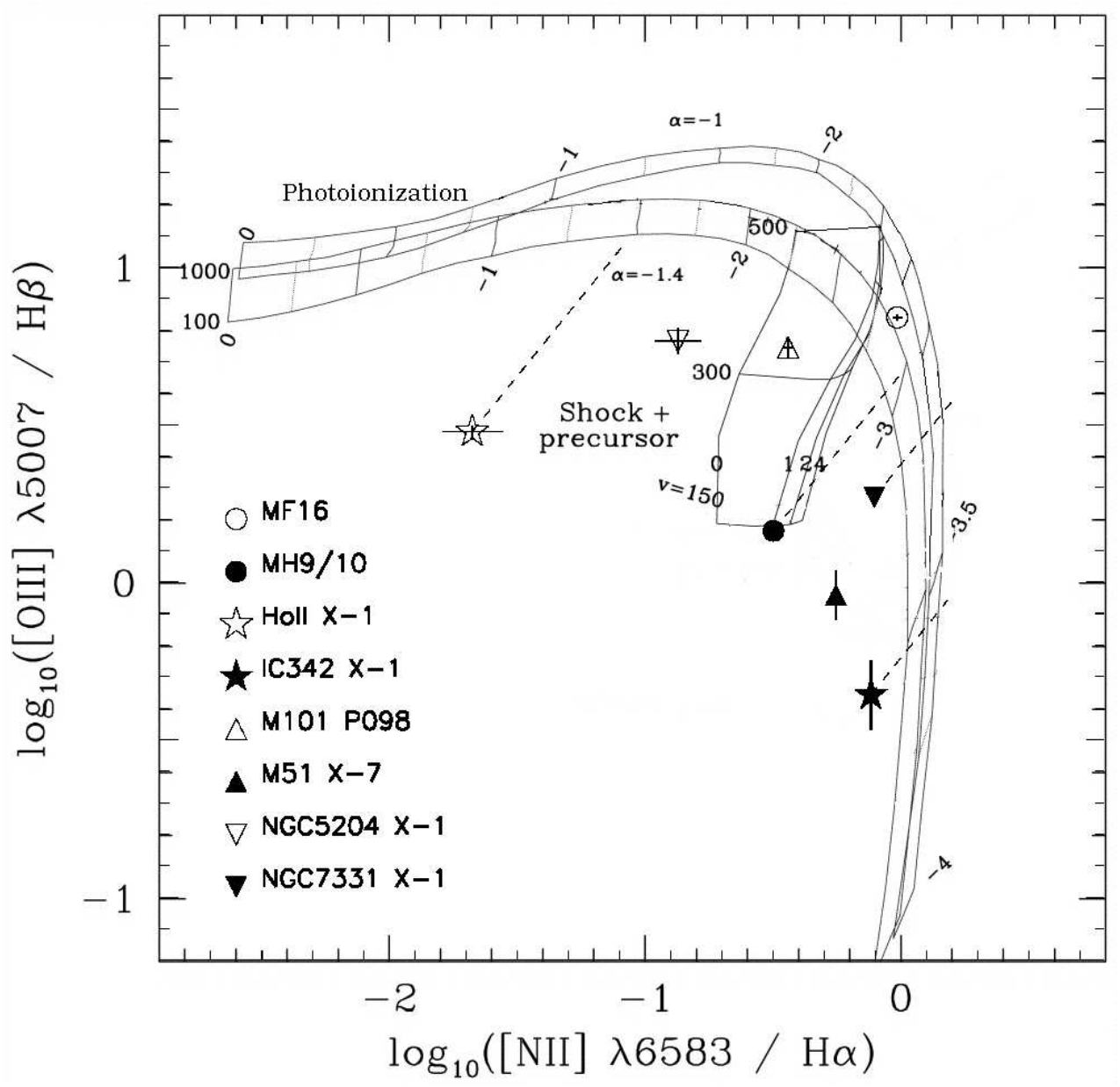

Figure 4: *Observed ULXNe on ionization diagram [NII]6583/Hα vs [OIII]λ5007/Hβ. Dotted lines indicate displacements from the observed position to that with solar abundance and the same physical conditions. Model grids are taken from the work of Evans et al.(1999). The longest curves stretching from the lower right to the upper left corner are MAPPINGsII photoionization models with a power-law source, labelled by logarithm of ionization parameter, ranging from -4 to 0, and by hydrogen density (100 and 1000 cm^{-3}, at the upper left corner). Shock+precursor MAPPINGsII models are shown labelled with the shock velocity in $km\,s^{-1}$ and magnetic parameter (0, 1, 2, 4, for details see Evans et al.(1999) and Allen et al.(1998)).*

lar population with StarBurst99 models (Leitherer et al., 1999; Vázquez & Leitherer, 2005) with solar and 0.4 of solar metallicities, and derived the best-fit age $T = 4.25 \pm 0.5\ Myr$ and the cluster mass $M \sim 40000 M_{\odot}$. The integral spectrum together with StarBurst99 best-fit stellar population and CLOUDY nebular spectra is shown in figure 8. WC features are bright in the spectrum, pointing to the presence of several WC stars. Emission line spectrum can not be totally explained by photoionization by the central cluster. Low-excitation shock-ionized lines like [S II]λ6717,6731 and [N II]λ6548,6583 have strong excess that can not be explained by the contribution from stellar winds and supernovae. We suggest that in this case the ULX is an additional source of mechanical power, comparable with the total luminosi-

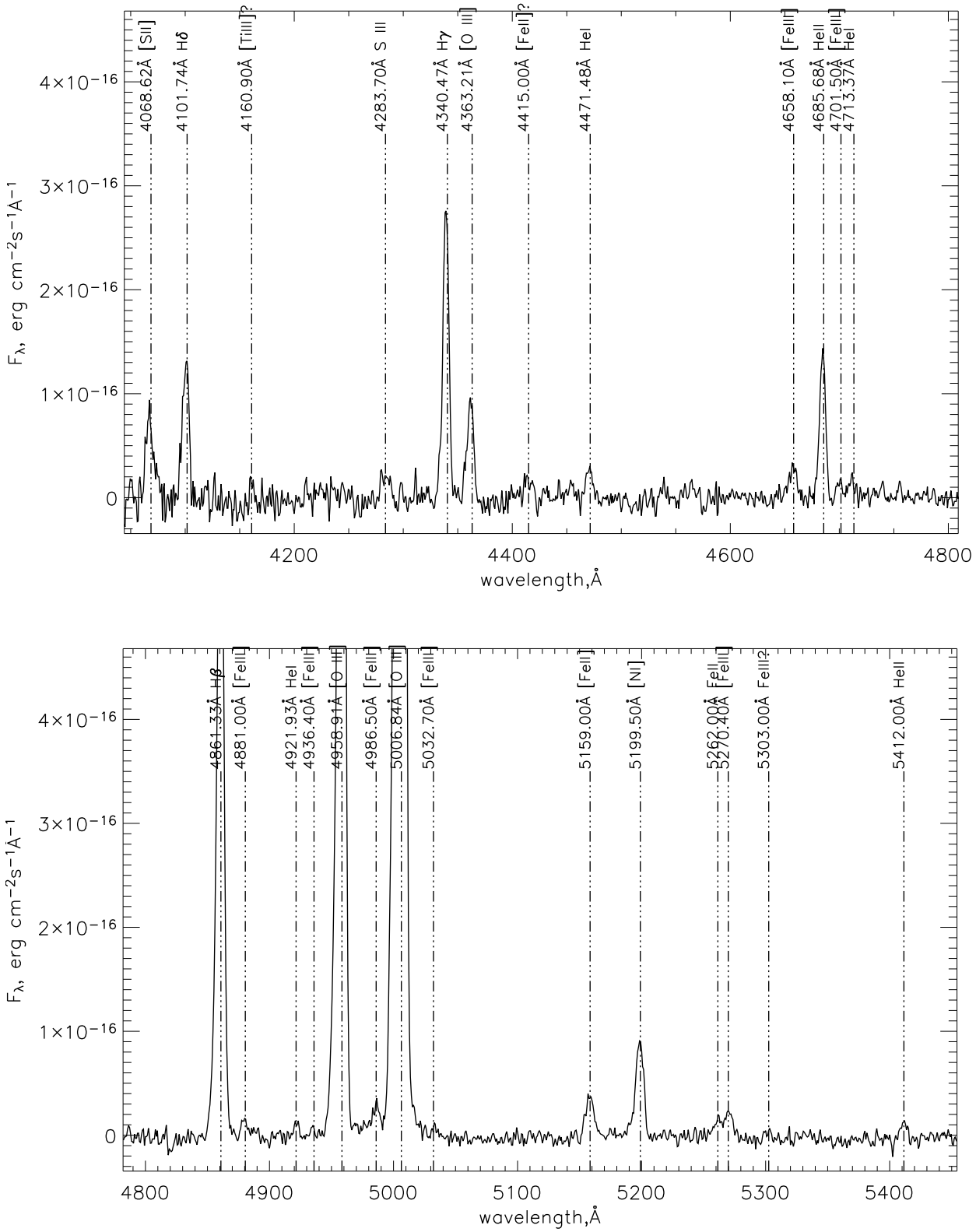

Figure 5: *Integral spectrum of MF16 (NGC6946 ULX-1 nebula) taken with SCORPIO.*

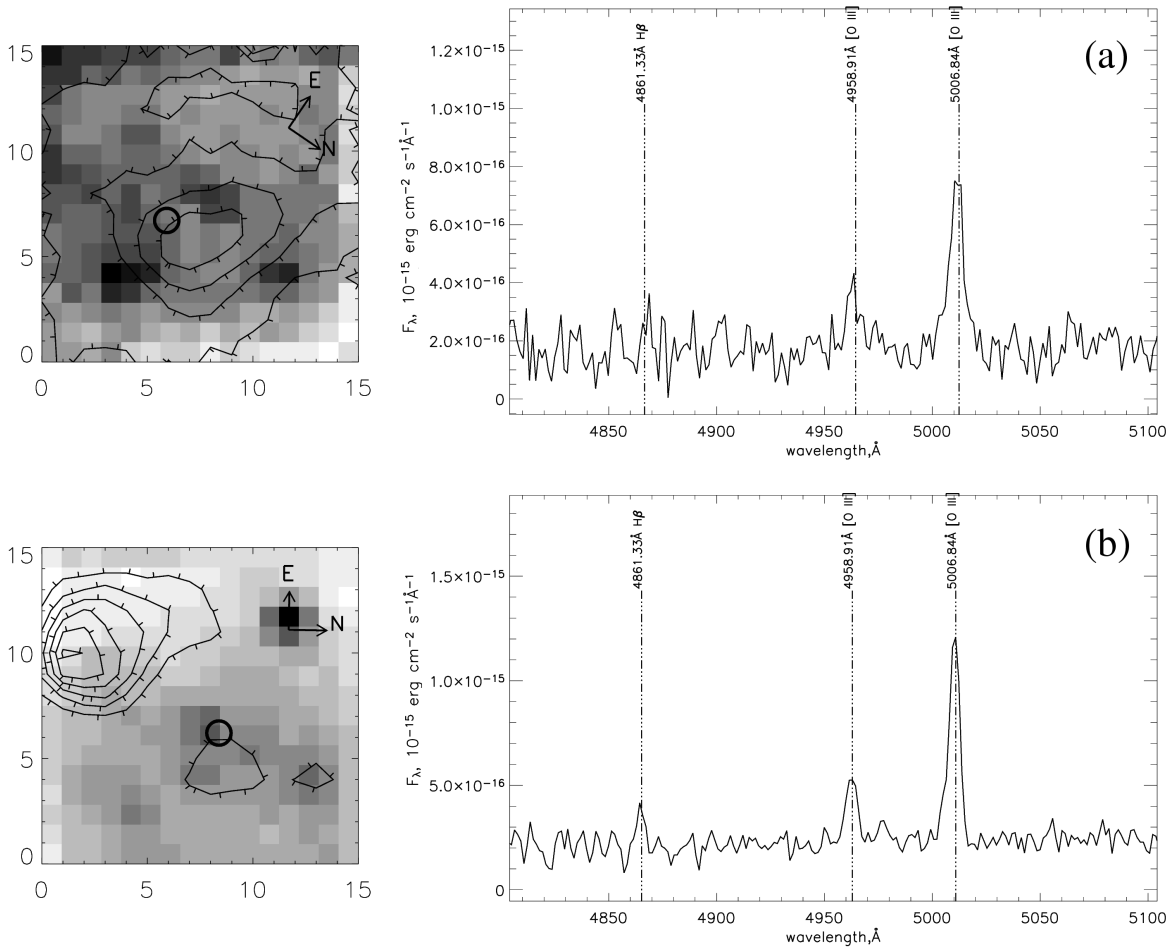

Figure 6: *High-excitation ULXNe in M101 (a) and NGC5204 (b) in* $16'' \times 16''$ *MPFS field. To the left continual flux maps in MPFS fields are shown overplotted with the [O III]λ4959,5007 flux contours. Here and below tick marks point towards lower intensity regions. To the right integral spectra of the [O III]-bright regions adjacent to the X-ray sources are shown. Chandra X-ray positions are shown by circles.*

ties of the brightest ULXNe like MF16. The residual emission line luminosities are given in brackets in table 2.

M51 X-7 is located at the outskirts of a bright star cluster (figure 9), clearly identified with a young massive cluster *n5194-839* from the list of Larsen (2000). It is a Super Star Cluster (SSC), or a young massive cluster, with the integral $M_V = -11\overset{\mathrm{m}}{.}09$ and $U - B = -0\overset{\mathrm{m}}{.}81$, indicating a rather young object of $T \sim 12\,Myr$. However, our spectral fitting with StarBurst99 models gives much larger cluster age $T \sim 60 \pm 15\,Myr$ and $A_V \sim 0\overset{\mathrm{m}}{.}5 \pm 0.1$. Most likely, stellar populations of different ages are seen in the vicinity of the X-ray source. Hα emission accompanied with bright [N II]λ6583,6548 and [S II]λ6717,6731 emission lines is coincident with the X-ray source within the spatial resolution. As emission line spectrum contains signatures of shock excitation we apply equation 3 for the estimate of the total power. A detail study of the M51 X-7 will be published in a separate paper.

4. Discussion

4.1. Metallicity and Oxygen Abundances

In table 2 we list oxygen abundance and metallicity estimates for the host galaxies and the ULX positions in the galaxies according to Pilyugin et al. (2003). It was argued by Soria (2006) that low metallicities can be crucial in understanding the nature of ULXs. Many of the objects are indeed found in subsolar metallicity environment, most likely at about 20-50% of solar metallicity. However, in our study of the star forming region associated with NGC7331 X-1 we find that solar-metallicity models provide better fit to the cluster spectrum that subsolar metallicity

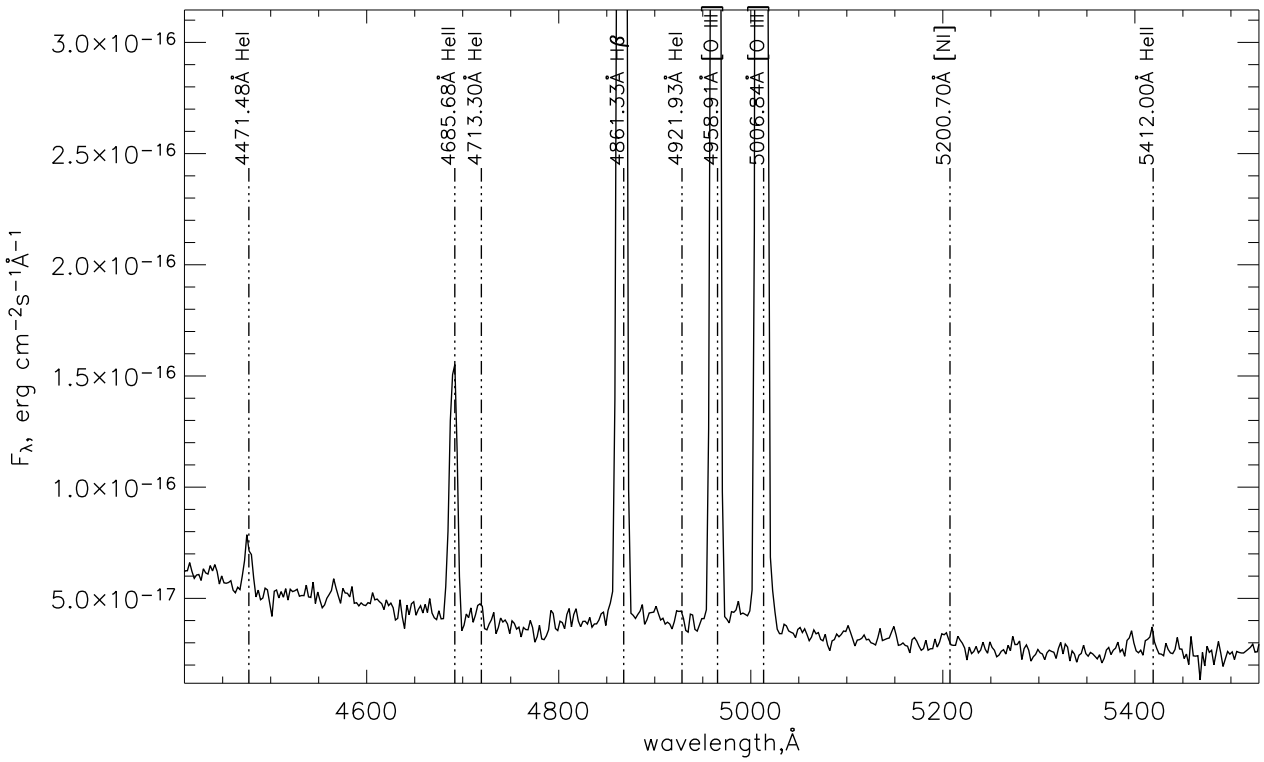

Figure 7: *Integral spectrum of the HoII X-1 nebula (Lehmann et al., 2005). Only part of the spectrum in 4500-5500Å spectral range is shown.*

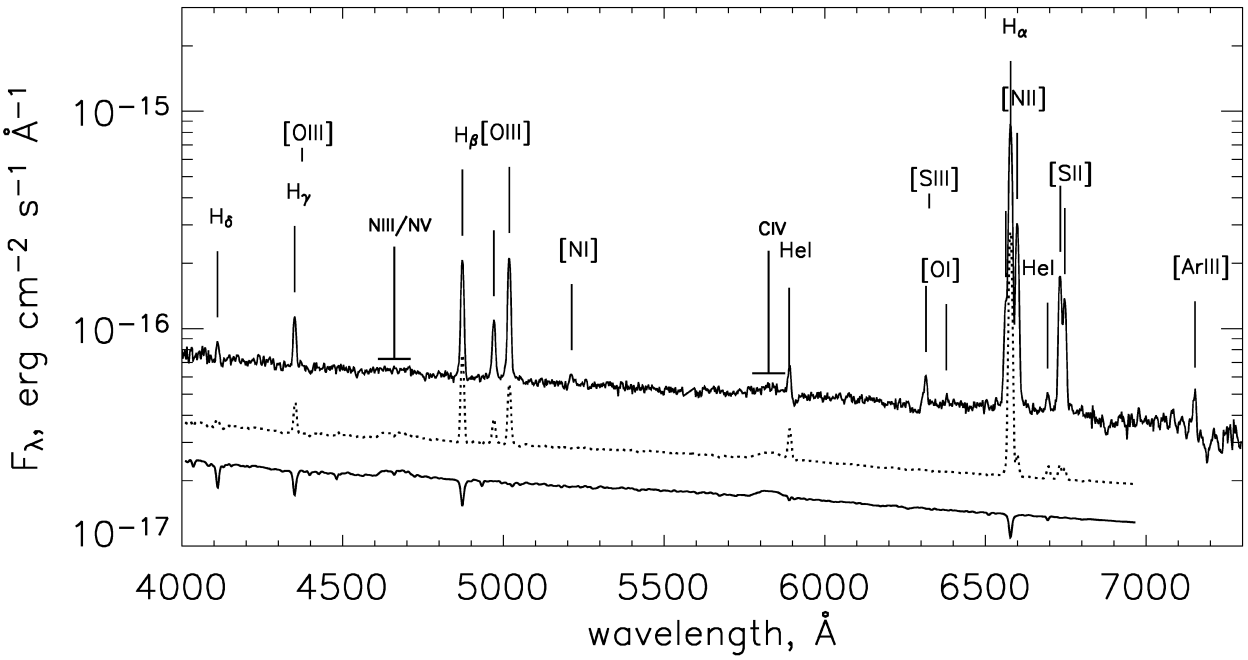

Figure 8: *Integral spectrum of the cluster in NGC7331 X-1 (upper solid), the best-fit StarBurst99 model (lower solid) and the best-fit StarBurst99 + best-fit nebular photoionization CLOUDY model spectrum. Model spectra are shifted in vertical direction.*

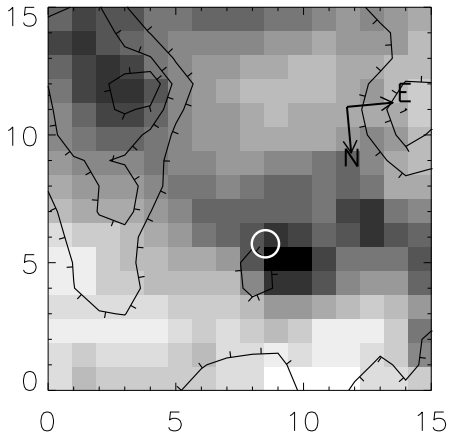

Figure 9: *M51 X-7* $16'' \times 16''$ *field observed with the MPFS. Stellar continuum integrated in the total spectral range is shown with the Hα countours overplotted. Chandra ULX position is marked by a white circle.*

models with $Z = 0.4Z_\odot$ and less.

In HII regions it is easier to estimate oxygen and nitrogen abundances rather than $[Fe/H]$. We can estimate oxygen abundance for some of our objects using the method of Pagel (1992), based on the similarity between oxygen and hydrogen ionization potentials. The method is based on the three-level atomic solutions by McCall (1984), allowing reliable calibrations of the ion abundances from their forbidden lines relative strengths. Oxygen abundance estimates use two relations for two ionization states of the element:

$$12 + \lg \frac{O^+}{H^+} = \lg \frac{I_{[OII]\lambda3726+\lambda3729}}{I_{H\beta}} + \\ + 6.174 + \frac{1.251}{t_3} - 0.55 \lg t_3$$

$$12 + \lg \frac{O^{++}}{H^+} = \lg \frac{I_{[OIII]\lambda4959+\lambda5007}}{I_{H\beta}} + \\ 5.890 + \frac{1.676}{t_2} - 0.40 \lg t_2 + \\ + \lg \left(1 + 1.35 \times 10^{-4} n_e t_2^{-1/2}\right),$$

where n_e is the electron concentration in cm^{-3}. t_3 and t_2 are the electron temperatures (in $10^4 K$ units) of the gas emitting in [O III] and [O II] lines, correspondingly. t_3 can be obtained from the characteristic line ratio $I_{[OIII]\lambda4959+\lambda5007}/I_{[OIII]\lambda4363}$ sensitive to electron temperature (Osterbrock, 1974). Because of the close ionization potential t_2 must be similar to the electron temperature estimate t_n made from another characteristic line ratio, $I_{[NII]\lambda6583+\lambda6548}/I_{[NII]\lambda5755}$. Usually, both [O II] and [O III] lines are present in a single H II region. Total abundance can be found by adding the ion abundances:

$$12 + \lg \frac{O}{H} \simeq 12 + \lg \left(\frac{O^+}{H^+} + \frac{O^{++}}{H^+} \right)$$

Unfortunately we do not detect [O II]λ3727 line in our spectra because of the limited spectral range for MPFS and sensitivity decrease for SCORPIO in the near UV range, so some additional assumptions will be needed.

For MF16 we have temperature estimates $t_3 = 1.9 \pm 0.1$ and $t_2 \simeq t_n = 1.5 \pm 0.2$, and $n_e \simeq 500 cm^{-3}$ derived from the sulfur doublet [S II]$\lambda6717, 6731$ components ratio. For MF16 oxygen abundance can not differ much from the solar, because both very bright [O III] and [O I] lines are well detected. For a very broad range of CLOUDY models (successfully predicting most of the observed line ratios) $I_{[OII]\lambda3726+\lambda3729}/I_{[OIII]\lambda4959+\lambda5007} \sim 1$. Using this estimate together with the directly observed value $I_{[OIII]\lambda4959+\lambda5007}/I_{H\beta} \simeq 9$, the temperature and density estimates one finds for MF16 $12 + \lg \frac{O}{H} \simeq 8.5$, i. e. practically solar abundance.

4.2. UV Sources

Point-like optical counterparts of ULXs are usually found as blue stars with $M_V \sim -5 \div -8^{\rm m}$ (Terashima et al., 2006). On the other hand, there are strong indications that at least some of the ultraluminous X-ray sources must be also ultraluminous EUV sources (in the range $20\mathring{A} \lesssim \lambda \lesssim 1000\mathring{A}$ responsible for hydrogen, oxygen and helium ionization). In the framework of the two most popular models (IMBH binaries and supercritical accretors), we can expect two explanations for the bright EUV radiation:

- Very massive ($M \gtrsim 10^4 M_\odot$) IMBH accreting at several percent of its Eddington level. Less massive IMBHs have too hard standard disk spectra. Note that the donor star contribution in the EUV region is most likely negligible.

- Supercritical accretion disk (SCAD) with stellar mass black hole and UV-radiating wind photosphere, like what we observe in SS433 (Fabrika, 2004).

IMBHs in binary systems are expected to have nearly-standard disks (because the accretion rates are most likely in the range $0.01 - 1.0$) with low outer temperatures. If the accretion disk in such system is tidally truncated by the secondary, its radius will be some fraction (roughly 0.5 of the black hole Roche lobe radius, practically equal to the binary separation, for example see Blondin (2000)) of the binary separation, that is $a \sim R_* \left(M_{BH}/M_*\right)^{1/3}$. This leads to at estimate of the outer disk temperature:

$$T_{out} \simeq 10^{-3} T_{in} \left(\frac{R_*}{10 R_\odot}\right)^{-3/4} \left(\frac{M_{BH}}{10^3 M_\odot}\right)^{-1} \left(\frac{M_*}{10 M_\odot}\right)^{-1}$$

In UV and optical ranges IMBH accretion disks have approximately power-law spectra with $F_\nu \propto \nu^{1/3}$ (Shakura & Sunyaev, 1973).

According to Poutanen et al. (2006), the temperature of the outer photosphere of a supercritical disk wind can be expressed as functions of the black hole mass in solar units m and mass accretion rate in Eddington units $\dot{m}$ as:

$$T_{ph} = \begin{cases} 0.2keV\ m^{-1/4}\dot{m}^{-1} & for\ v \propto r^{-1/2} \\ 0.8keV\ m^{-1/4}\dot{m}^{-3/4} & for\ v = const, \end{cases} \quad (6)$$

where v is the radial velocity of the outflowing wind forming inside of the spherization radius, $v \propto r^{-1/2}$ corresponds to the case when the velocity is everywhere proportional to the virial, and $v = const$ is the case of a relatively fast wind. m is the black hole mass in Solar units, $\dot{m}$ is the mass accretion rate in Eddington units.

For accretion rates $\dot{m} \sim 10 - 100$ maximum of the photosphere radiation falls in a spectral range of hundreds of angstroms. Expected total photosphere luminosity is $\sim 10^{39} \div 10^{40}$ergs s^{-1}.

In figure 10 we present spectral energy distributions (SEDs) for multicolor accretion disk (Shakura & Sunyaev, 1973; Mitsuda et al., 1984) models for IMBHs and SCAD photospheres with different black body temperatures. The NGC6946 ULX-1 SED inferred from optical and X-ray observations is also presented. The SED of NGC6946 ULX-1 looks fairly flat compared with blackbody and MCD models. This can be explained qualitatively by a supercritical accretor system spectrum (Fabrika et al., 2007): the disk funnel ($\sim 10^{39} - 10^{40}$ ergs s^{-1}in X-ray band), the wind photosphere ($\sim 10^{39} - 10^{40}$ ergs s^{-1}in EUV/UV) and the donor star ($\sim 10^{38}$ ergs s^{-1}in the optical/UV).

If ULXs are indeed supercritical accretors one may expect a wide range of X-ray luminosities and photosphere temperatures, resulting in large variety of UV/EUV properties practically independent of the X-ray spectrum. For $\dot{m} \sim 100$ a bright EUV source and a photoionized nebula are likely to appear. For $\dot{m} \lesssim 10$, however, one can expect only a compact HII region with relatively bright high-excitation lines like He IIλ4686 and [O III]λ5007. This is probably the case for HoII X-1 and M101 P098. Very large accretion rates ($\dot{m} > 1000$) result in a very soft photosphere emission combined with X-ray ionization and strong wind producing a large shock-powered nebula.

As can be seen from figure 10 ULXs are reachable sources for *GALEX* (Martin et al., 2003). For sources with lower absorption even UV spectroscopy will be possible in pointing observations. The main predicted difference between SCADs and IMBHs in the UV is in the difference of the spectral slopes in these two models. We also expect SCADs to be more divergent spectral properties in the UV range.

5. Conclusions

We confirm that ULXs belong to young stellar population. Some of them are certainly formed in star clusters and associations of 5-10 Myrs old. Most of ULXs are surrounded with nebulae. Studying the nebulae gives us a powerful tool to investigate the nature of ULXs. At least 4 (group A) of 8 ULXNe studied in this paper show high flux ratio [O III]λ5007/Hβ = $3 \div 7$ (table 2), that requires a strong EUV source (ultraluminous UV sources, UUVs) to ionize the nebula. Other 4 of the 8 ULXNe (group B) are most likely shock-ionized.

There is a ULXN in the group B, the nebula of NGC7331 X-1. Abolmasov et al. (2007b) have found parameters of the young super-stellar cluster (SSC) hosting the ULX and calculated the nebula spectrum using CLOUDY photoionized by the SSC in NGC7331. Residual emission line spectrum (values in brackets in table 2), obtained after subtraction of the model spectrum from the observed spectrum, it shows both enhanced shock-excited lines (like [S II]λ6717,6731) and [O III]λ4959,5007 doublet relative to the total emission-line spectrum of the cluster HII region. The residual spectrum of the nebula in NGC7331 is quite similar to spectrum of MF16, but about twice as fainter. NGC7331 X-1 residual emission may be a fainter equivalent of MF16.

Signatures of high excitation (He II, [Fe III], [O III]lines) are present in most of the spectra. Low-excitation shock-excited lines are unusually bright in the spectra of ULNXe as well. We isolate then a group A (HoII X-1, NGC6946 X-1, M101 Po98 and NGC5204 X-1) requiring a strong EUV source to ionize oxygen and a group B (HoIX X-1, IC342 X-1, NGC7331 X-1 and M51 X-7) having higher ratios [SII]λ6717, 6731/Hβ = $2.3 - 4$ and requiring shock excitation of their nebulae. We note that in fact *all the ULXNe* studied in the paper show the shock excitation, because their ratios [SII]λ6717, 6731/Hα = $0.3 - 1.1$.

We may make (preliminary) conclusions:

— All the ULXNe show signatures of shock excitation, however the local ISM environment can also change the appearance of a ULX nebula.

— Half of the ULXNe (the group A) require additional strong EUV continua (ultraluminous UV sources, UUVs) to ionize the nebulae.

However, this isolation of A and B groups may be done only in average. For example, IC342 X-1 nebula (the group B) shows that the central parts of the nebulae is bright in high-excitation lines. In fact all the ULXNe except two (M51 X-7 and NGC7331 X-1 residual emission) show either HeII λ4686 emission or enhanced [O III]λ4959,5007 / Hβ ratio which indicate the presence of hard ionizing source with the

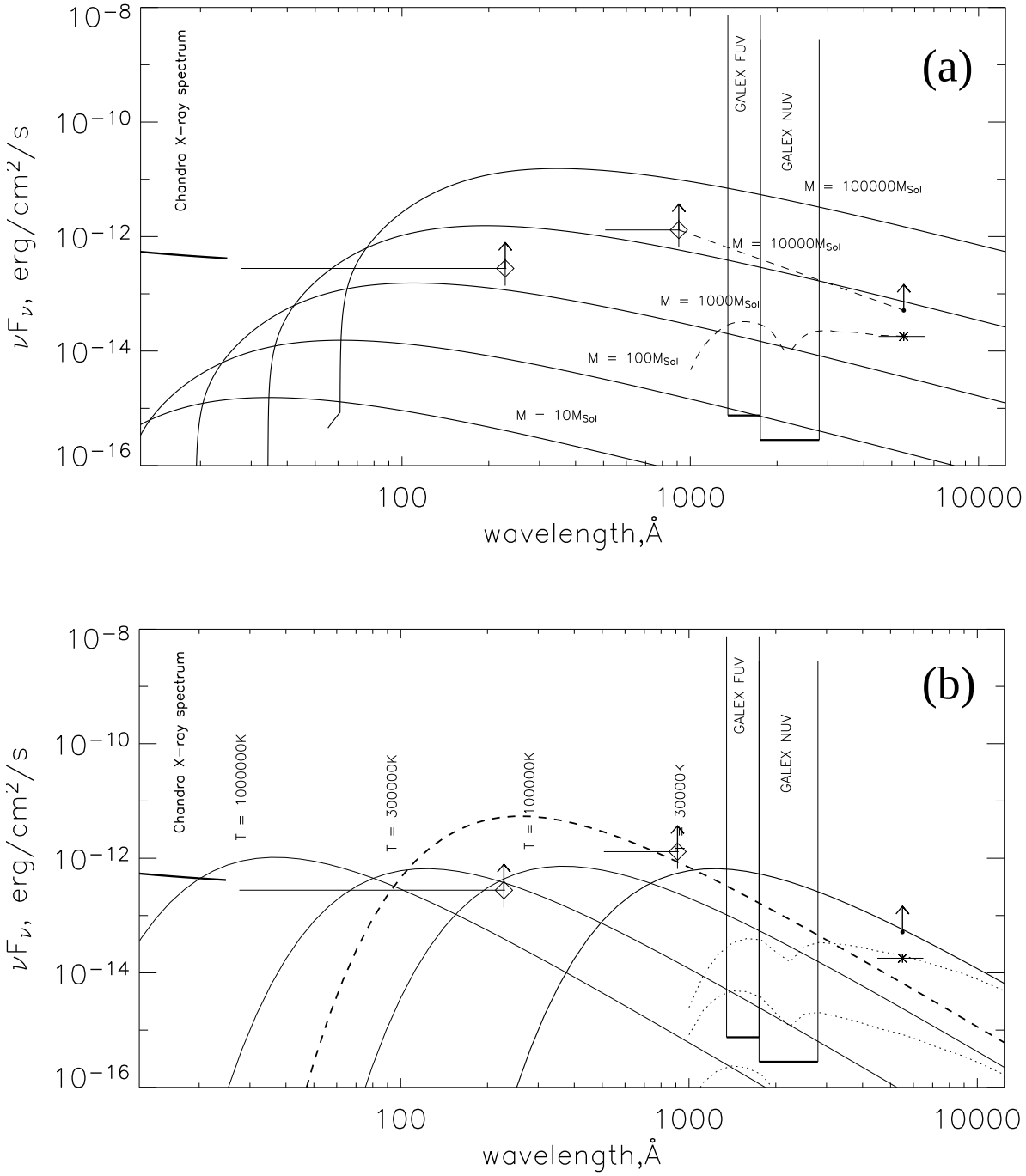

Figure 10: *Spectral energy distribution from the X-rays to the optical range derived for NGC6946 X-1. Optical source (star d, the V-band flux) is indicated by an asterisk, the upward arrow is the value corrected for the Galactic absorption (it is a lower limit because of possible intrinsic absorption). Two diamonds with bars ranging towards higher energies are the estimates for the EUV luminosity based on the optical emission-line luminosities of MF16 (HI and HeII lines, the symbols mark HI and HeII Lyman edges). The X-ray spectrum is represented by the best-fit model for the Chandra data given by Roberts & Colbert (2003). In two GALEX bands the limiting fluxes are shown with the $S/N = 3$ detection limit for exposure time $t = 10^5 s$. (a) MCD models for black holes accreting at $0.01\dot{M}_{Edd}$ are shown with solid curves. Dashed lines show both a power-law interpolation between hydrogen edge and V-band, and the same spectrum, but reddened by Galactic absorption (Cardelli et al.(1998) reddening curves were used). (b) Black body models with $L = 10^{39} ergs\ s^{-1}$ are presented, together with the optimal blackbody model for the UV radiation obtained in CLOUDY modelling. Dotted curves*

luminosity $\sim 10^{38}$ergs s^{-1}. Most likely shock waves, X-ray and EUV ionization act simultaneously in all the ULXNe, but the relative importance of the power sources varies significantly.

In some ULXNe radial velocity gradients ($\sim$100 km/s) were directly detected (Dunne et al.(2000), Pakull et al.(2006), Fabrika et al.(2006) and references therein). We make an additional conclusion:

— ULXs must produce strong winds and/or jets powering their nebulae with $\gtrsim 10^{39}$ergs s^{-1}. This is consistent with the suggestion that ULXs are high-mass X-ray binaries with the supercritical accret of the SS433 type. From the other hand, accreting IMBHs with standard disks are unlikely to have jet or wind activity.

Some of ULXs are bright ultraviolet sources with hydrogen- and helium-ionizing luminosities varying from $\sim 10^{38}$ to $\sim 10^{40}$ergs s^{-1}. This property can be still explained by a population of IMBHs with comparatively high ($\sim 10000 M\odot$) masses or stellar-mass supercritical accretors (SCAD) like SS433. Future UV (Galex) observations may help in solving of this task, we predict different spectral slopes in the UV spectral ranges in the IMBHs/SCADs models.

Acknowledgements. This work was supported by the RFBR grants NN 05-02-19710, 04-02-16349, 06-02-16855.

References

Abolmasov, P., Fabrika, S., Sholukhova, O. & Afanasiev, V. 2006 in Science Perspectives for 3D Spectroscopy, ed. M. Kissler-Patig, M. M. Roth. & J. R. Walsh (Springer Berlin / Heidelberg); astro-ph/0602369

Abolmasov, P., Fabrika, S., Sholukhova, O. & Afanasiev, V. 2007 *in preparation*

Abolmasov, P., Swartz, D., Fabrika, S. et al.2007 *in preparation*

Abramowicz, M. A., Calvani, M., Nobili, L. 1980, Astrophys. J., **242**, 772

Afanasiev V.L., Dodonov S.N., Moiseev A.V., 2001, in *Stellar dynamics: from classic to modern*, eds. Osipkov L.P., Nikiforov I.I., Saint Petersburg, 103

Afanasiev, V. & Moiseev, A. 2005, Astronomy Letters, **31**, 194

Allen M. G., Dopita, M. A., Tsvetanov, Z. I. 1998, Astrophys. J., **493**, 571

Begelman, M. C. 2002, Astrophys. J., **568**, L97

Blair, W. P., Fesen, R. A. & Schlegel, E. M. 2001, Astron. J., **121**, 1497

Blondin, J. 2000, New Astronomy, **5**, 53

Braun, R. & Walterbos, R. A. M. 1993, Astron. Astrophys. Suppl. Ser., **98**, 327

Cardelli, J. A., Clayton, G. C. & Mathis, J. S. 1998, Astrophys. J., **345**, 245

Colbert, E. J. M., Miller, E. C. 2005 astro_ph/0402677

Coluzzi, R. 1996 Bull. Inf. Centre Donnees Stellaires, **48**, 15

Conty, P.S., Leep, M.E. & Perry, D.N. 1983, Astrophys. J., **268**, 228

Copperwheat, C., Cropper, M., Soria, R., Wu, K. 2005, Mon. Not. R. Astron. Soc., 362, 79

Dopita, M. A. & Sutherland, R. S. 1996, Astrophys. J. Suppl. Ser., **102**, 161

Dunne, B. C., Gruendl, R. A., Chu, Y.-H. 2000, AJ, **119**, 1172

Evans, I., Koratkar, A., Allen, M., Dopita, M., Tsvetanov, Z. 1999 Astrophys. J., **521**, 531

Fabrika, S., Mescheryakov A. 2001. In: *Galaxies and their Constituents at the Highest Angular Resolution*, IAU Symp. N205, ed. R.T. Schilizzi, p. 268

Fabrika, S., 2004, Astrophys. and Space Phys. Rev., 12, 1

Fabrika, S., Karpov, S., Abolmasov, P. & Sholukhova, O. 2006. In Populations of High Energy Sources in Galaxies, IAU Symposium 230, ed. E. J. A. Meurs & G. Fabbiano, p. 278; astro-ph/0510491

Feldmeier, J. J., Ciardullo, R., Jacoby, G. H. 1997, Astrophys. J., **479**, 231

Ferland, G. J., Korista, K.T., Verner, D.A., Ferguson, J.W., Kingdon, J.B. & Verner, E.M. 1998,Publ. Astr. Soc. Pacific, **110**, 761

Ferrarese, L., Mould, J. R., Kennicutt, R. C., et al. 2000, Astrophys. J., **529**, 745

Goad, M. R., Roberts, T. P., Knigge, C., & Lira, P. 2002, MNRAS, **335**, 67

Grisé, F., Pakull, M. W. & Motch, C. 2006, in Populations of High Energy Sources in Galaxies, IAU Symposium 230, ed. E. J. A. Meurs & G. Fabbiano, p. 302; astro-ph/0603768

Helfand, D. J. 1984, Publ. Astr. Soc. Pacific, **96**, 913

Hopman, C., Portegies Zwart, S. F.. Alexander, T. 2004, Astrophys. J., **604**, 101L

Hughes, S. M. G., Han, M., Hoessel, J. et al.1998, Astrophys. J., **501**, 32

Kaaret, P., Ward, M. J., & Zezas, A. 2004, MNRAS, 351, 83

Karachentsev, I. D., Dolphin, A. E., Geisler, D., Grebel, E. K., Guhathakurta, P., Hodge, P. W., Karachentseva, E. V., Sarajedini, A., Seitzer, P., Sharina, M. E. 2002, A& A, 383, 125

Fabrika, S., Karpov, S., Abolmasov, P. 2007, *in preparation*

King, A.R., Davies, M.B., Ward, M.J., Fabbiano, G., Elvis, M. 2001, Astrophys. J.Letters, **552**, 109

Krauss, M. I., Kilgard, R. E., Garcia, M. R., Roberts, T. P., Prestwich, A. H. 2005 Astrophys. J., **630**, 228

Kuntz, K. D., Gruendl, R. A. & Chu, Y.-H. et al. 2005 Astrophys. J., **620**, 31

Larsen, S. S. 2000, Mon. Not. R. Astron. Soc., **319**, 839

Lehmann I., Becker T., Fabrika S. et al. 2005, Astron. Astrophys., **431**, 847

Leitherer, C., Schaerer, D., Goldader, J. D. et al. 1999, Astrophys. J. Suppl. Ser., **123**, 3

Liu, J.-F., Bregman, J. N., Seitzer, P. 2004, Astrophys. J., **602**, 249L

Long, K. S. & van Speybroeck, L. P. 1983, Accretion Driven Stellar X-ray Sources, ed. W. H.G. Lewin, & E. P.J. van den Heuvel (Cambridge: Cambridge University Press), 141

Madau, P., Rees, M. J. 2001, Astrophys. J., **551**, L27

Makarova, L. N., Grebel, E. K., Karachentsev, I. D. et al.2002, A& A, **396**, 473
Martin, C., GALEX Science Team 2003, Bulletin of the American Astronomical Society, **35**, 1363
Mescheryakov, A. 2004 private communication
Miller, B. W. 1995 Astrophys. J., **446**, L75
Mitsuda, K., Inoue, H., Koyama, K., Makishima, K., Matsuoka, M., Ogawara, Y., Suzuki, K., Tanaka, Y., Shibazaki, N., Hirano, T. 1984, PASJ, **36**, 741
Osterbrock, D. E. "Astrophysics of Gaseous Nebulae" 1974, San Francisco, eds. W. H. Freeman and Company
Pagel, B. E. J., Simonson, E. A., Terlevich, R. J., Edmunds, M. G. 1992, Mon. Not. R. Astron. Soc., **225**, 325
Pakull, M.W. & Mirioni, L. 2003, in: "Winds, Bubbles, and Explosions: a conference to honor John Dyson", RevMexAA (Serie de Conferencias) 15, 197, ed. J. Arthur & W. J. Henney
Pakull, M.W., Grisé, F., Motch, C. 2006, in: "Populations of High Energy Sources in Galaxies": IAU Symposium 230, ed. E. J. A. Meurs & G. Fabbiano, p. 293; astro-ph/0603771
Petit, H. 1998, Astron. Astrophys. Suppl. Ser., **131**, 317
Pilyugin, L. S., Thuan, L. X. & Vílchez, J. M. 2003, Astron. Astrophys., **397**, 487
Poutanen, J., Fabrika, S., Butkevich, A., Abolmasov, P. 2006 *in press*
Regan, M. W., Thornley, M. D., Bendo, G. J. et al. 2004 Astrophys. J. Suppl. Ser., **154**, 204
Roberts, T. P., Colbert, E. J. M. 2003 Mon. Not. R. Astron. Soc., **341**, 49
Roberts, T. P., Goad, M. R., Ward, M. J., Warwick, R. S. 2003, Mon. Not. R. Astron. Soc., **342**, 709
Saha, A., Claver, J., Hoessel, J. G. 2002, Astron. J., **124**, 839
Schlegel, D. J., Finkbeiner, P. F., Davis, M. 1998, Astrophys. J., **500**, 525
Shakura, N. I., Sunyaev, R. A. 1973, Astron. Astrophys., **24**, 337
Soria, R., Cropper, M., Pakull, M., Mushotzky, R., Wu, K. 2005, Mon. Not. R. Astron. Soc., **356**, 12
Soria, R., Fender, R. P., Hannikainen, D. C., Read, A. M. & Stevens, I. R. 2006, Mon. Not. R. Astron. Soc., **368**, 1527
Soria, R. 2006, astro_ph/0509573
Swartz, A. D., Ghosh, K. K., Tennant, A. F. & Wu, K. 2004, Astrophys. J. Suppl. Ser., **154**, 519
Stetson, P. B., Saha, A., Ferrarese, L. et al.1998, Astrophys. J., **508**, 491
Terashima, Y., Inoue, H., Wilson, A. S. 2006, Astrophys. J., **645**, 264
Tully, R. B., **1988**, "Nearby Galaxies Catalog" Cambridge: Cambridge Uni- versity Press
Tully, R. B., Shaya, E. J., Pierce, M. J. 1992, Astrophys. J. Suppl. Ser., **80**, 479
Vázquez, G. A. & Leitherer, C. 2005, ApJ, **621**, 695
Zezas, A., Fabbiano, G., Rots, A. H., Murray, S. S. 2002, Astrophys. J., **577**, 710